Experimental Study of Damage Indicators for a 2-Bay, 6-Storey RC-Frame

Skjærbæk, P. S.; Nielsen, Søren R. K.; Kirkegaard, Poul Henning; Cakmak, A. S.

Publication date:
1997

Document Version
Early version, also known as pre-print

INSTITUTTET FOR BYGNINGSTEKNIK
DEPT. OF BUILDING TECHNOLOGY AND STRUCTURAL ENGINEERING
AALBORG UNIVERSITET • AAU • AALBORG • DANMARK

FRACTURE & DYNAMICS
PAPER NO. 87

Submitted to Journal of Structural Engineering, ASCE

P.S. SKJÆRBÆK, S.R.K. NIELSEN, P.H. KIRKEGAARD, A.Ş. ÇAKMAK
EXPERIMENTAL STUDY OF DAMAGE INDICATORS FOR A 2-BAY, 6-STOREY RC-FRAME

AUGUST 1997 ISSN 1395-7953 R9725

The FRACTURE AND DYNAMICS papers are issued for early dissemination of research results from the Structural Fracture and Dynamics Group at the Department of Building Technology and Structural Engineering, University of Aalborg. These papers are generally submitted to scientific meetings, conferences or journals and should therefore not be widely distributed. Whenever possible reference should be given to the final publications (proceedings, journals, etc.) and not to the Fracture and Dynamics papers.

Printed at Aalborg University

Experimental Study of Damage Indicators for a 2-Bay, 6-Storey RC-Frame

P.S. Skjærbæk[1], S.R.K. Nielsen[1], P.H. Kirkegaard[1] and A.Ş. Çakmak[2]

[1] Department of Building Technology and Structural Engineering, Aalborg University, DK-9000 Aalborg, Denmark

[2] Department of Civil Engineering and Operations Research, Princeton University, Princeton, NJ 08544, USA

Abstract A 2-bay, 6-storey model test RC-frame (scale 1:5) subjected to sequential earthquakes of increasing magnitude is considered in this paper. Based on measured storey accelerations and ground surface accelerations several methods for assessment of damage including the global maximum softening damage index, Park and Ang's index, the normalized cumulative dissipated energy, various ductility ratios, a low-cycle fatigue model formulated by Stephens, the flexural damage ratio, interstorey drift based damage ratios and a newly proposed local maximum softening damage index are used. Like the maximum softening damage index the latter index is estimated from slowly time-varying eigenfrequencies. After the last earthquake the model test frame is cut in smaller pieces which are exposed to different static loads to evaluate the stiffness deterioration of the different beams and columns for a more precise evaluation of the final damage of the structure. The various damage indicators are then compared and it is concluded that some divergence between the indicators is found.

Introduction

Experiences from past earthquakes in the last decades have shown a growing need for methods to localize and quantify damage sustained by RC-structures during earthquakes. Traditional visual inspection can be used to locate and measure the damage state of an RC-structure. However, a much more attractive method is to measure the dynamic response of the structure at one or more positions and from this information estimate the damage state of the structure. During the last 10-20 years much research has been performed within this area and many different methods for damage assessment have been suggested in the literature. Almost all of the proposed methods are based on calculating a socalled damage index, which is supposed to reflect the damage state of the considered structure, substructure or structural member. Unfortunately many of the suggested damage indices do not have a well defined mapping of the numerical value to a certain damage state, and the mapping of some of the indices has shown a significant dependence on the considered structure which makes the index difficult to use for damage assessment. The requirements for a good damage assessment method can therefore be formulated as follows, se e.g. Stephens [19]:

1. The index should have general applicability, i.e. it should be valid for a variety of structural systems.

2. It should be based on a simple formulation and be easy to use.

3. It should generate easily interpretable results.

The purpose of this paper is to investigate how the proposed methods for damage assessment of RC-structures suggested in the literature work when applied to a scale 1:5 model test reinforced concrete frame subjected to ground acceleration time-series of increasing magnitude. The investigations are performed on acceleration response measurements from shaking table tests with a 2-bay, 6-storey model test RC-frame.

The considered data are sampled from a model structure tested at the Structural Dynamics Laboratory at Aalborg University during the autumn of 1996.

Damage Indices

Due to the large number of damage indices (DI)s suggested in the literature and the obvious correlation between some of those, the aim is to consider here a limited number of these containing all basic measures of damage. A more throrough overview of the damage indices suggested in the literature can be found in Stephens [19] or more recently in Williams et al. [23]. It should be noted, that the formulation presented in the following presumes that the methods are devised for assessment of storey damage or global damage in a framed structure.

Interstorey Drift (ID)

Damage indices based on interstorey drifts have been proposed in various formulations by Culver et al. [3], Toussi and Yao [22], Sozen [18] and Roufaiel and Mayer [15]. The index based on interstorey drift considered here is due to Toussi and Yao, who defined their index for the ith storey as the ratio between the maximum interstorey displacement $u_{\max,i}$ of storey i and the storey height h as

$$ID_i = \frac{u_{\max,i}}{h} \tag{1}$$

From studies of test data of structural components and small-scale structures, it was found that ID_i equal to 1% corresponds to damage of non-structural components while values larger than 4% represent irrepairable damage or collapse.

Ductility Ratio (DR)

The ductility of a structure or a member of a structure is defined as its ability to deform inelastically without total fracture or substantial loss of strength. In the literature it is common use to express these deformation demands in terms of a ductility ratio DR, calculated as the ratio of maximum deformation to deformation at first yield. The DR is used directly as a damage measure where the critical value is a material parameter. The maximum deformation is determined from the load-deformation history of the considered structure. The deformation considered can be of all kinds, curvature, rotation, displacement, strain in a member etc. At structural level displacements are used, and the DR will then be expressed as a displacement ductility ratio defined as

$$DR_i = \frac{u_{\max,i}}{u_{y,i}} \tag{2}$$

Where $u_{y,i}$ is the yielding interstorey displacement.

Ductility ratios have been used extensively in seismic analysis to evaluate the capacity of structures undergoing inelastic deformations, Rahman and Grigoriu [14]. However, as damage index, the ductility ratio often performs unsatifactorily because it cannot account for both duration and frequency content of typical ground motions, Banon and Veneziano [2]. Furthermore, the use of the DR is limited by the fact that determination of response at yielding of an element or structure is difficult. The interpretation of this kind of damage index is also a problem since the critical value of the ductility ratio is varying from structure to structure.

Normalized Cumulative Deformations (NCD) and Dissipated Energy (NDE)

Banon et al. [1] defined a damage index based on cumulative plastic deformation as the sum over all n half-cycles of all maximum plastic interstorey deformations at the ith storey in proportion to $u_{y,i}$.

$$NCD_i = \sum_{j=1}^{n} \frac{|u_{p,j}|_i}{u_{y,i}} \tag{3}$$

Normally the maximum plastic deformation in a half-cycle is calculated as the displacement at zero force in the force-deformation curve. Generally no rule has been developed for mapping values of this index to an actual damage state of the structure.

Along with the normalized cumulative deformations Banon et al. [1] also suggested the normalized cumulative dissipated energy to be used as a damage index, which was defined as the ratio of the energy dissipated in inelastic deformation to the maximum elastic energy that can be stored in the member in anti-symmetric bending

$$NDE_i = \int_0^t \frac{2P_i(\tau)du_i(\tau)}{P_{y,i}u_{y,i}} \tag{4}$$

$P(\tau)$ is the shear force at the time τ and $P_{y,i}$ is the yield force for the ith storey. As for the cumulative deformations, a rule for mapping values of the index into a specific damage state is lacking.

Flexural Damage Ratio (FDR)

In another suggestion, Banon et al. [1] correlated the damage to the ratio of initial interstorey shear stiffness $K_{i,i}$ to the reduced secant stiffness $K_{RS,i}$ at the maximum displacement in the socalled Flexural Damage Ratio

$$FDR_i = \frac{K_{i,i}}{K_{RS,i}} \tag{5}$$

The parameters entering the definition of the Flexural Damage Ratio is calculated as illustrated in figure 1.

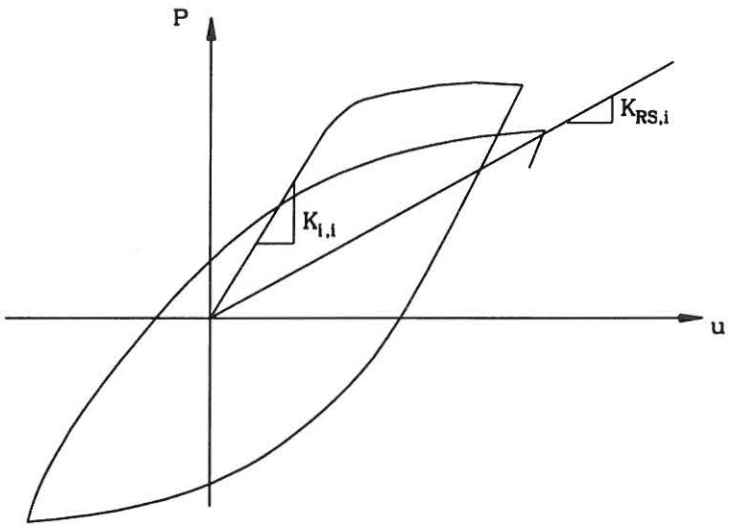

Figure 1: Definition of flexural damage ratio.

Stephens' Extended Index (SEI)

Stephens [19] defined a cumulative plastic deformation damage index where the damage sustained during the jth half-cycle of response is determined as

$$\Delta d_{j,i} = \left(\frac{u^+_{j,i}}{u^+_{f,j,i}} \right)^{\alpha} \tag{6}$$

where $u^+_{j,i}$ is the change in positive plastic interstorey deformation, $u^+_{f,j,i}$ is the change in positive plastic interstorey deformation leading to failure in a one-cycle test conducted at the relative deformation ratio, rl, of cycle j. The relative deformation ratio is defined as the ratio of the change in negative plastic interstorey deformation in cycle j, $u^-_{j,i}$, to the change in positive plastic interstorey deformation in cycle j. α is a fatigue damage exponent given as $\alpha = 1-(b \cdot rl)$. Stephens suggested the value $b = 0.77$ to be used for RC-components. The parameters in Stephens' index are defined in figure 2.
The total damage of the ith storey is then obtained by linear summation of the damage contribution of all half-cycles.

$$SEI_i = \sum_{j=1}^{n} \Delta d_{j,i} \tag{7}$$

Park and Ang's Index (PA)

Park and Ang's [12] index combines the contributions from maximum deformation damage and from dissipated energy as

$$PA_i = \frac{u_{\max,i}}{u_{u,i}} + \frac{\beta}{P_{y,i} u_{u,i}} \int dE_i \tag{8}$$

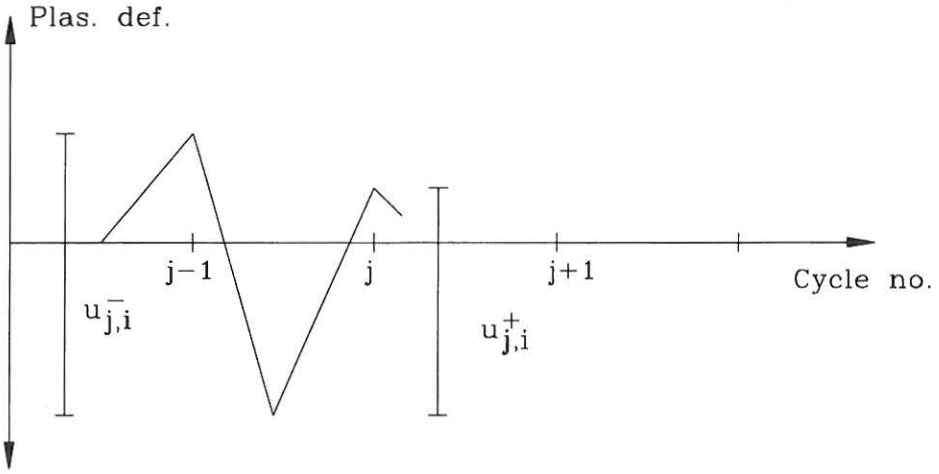

Figure 2: Definition of parameters in Stephens' index.

where $u_{u,i}$ is the ultimative interstorey deformation under monotonic loading, dE_i is the incremental dissipated energy and β is a non-negative strength deterioration parameter, which on average has been found to be 0.25. On average it is supposed that a value of 1 of this index corresponds to collapse.

The Maximum Softening Damage Index (MSDI)

The maximum softening concept is based on the variation of the vibrational periods of a structure during a seismic event. A strong correlation has been documented between the damage state of a reinforced concrete structure that has experienced earthquake and the global maximum softening $MSDI$. In order to use the maximum softening as a measure of the damage of the structure it is necessary to establish a quantitative relationship between the numerical value of the maximum softening and engineering features of damage. This relationship is obviously very complicated and has to be found by measurement from real structures by regression analysis. DiPasquale et al. [4] investigated a series of buildings damaged during earthquakes and found a very small variation coefficient for the maximum softening damage index, see figure 3. Nielsen and Çakmak [9] extended the maximum softening to substructures based on a multidimensional maximum softening $MSDI_i$ defined as

$$MSDI_i = 1 - \frac{T_{i,0}}{T_{i,\max}} \tag{9}$$

Where $T_{i,0}$ is the initial value of the ith eigenperiod for the undamaged structure and $T_{i,\max}$ is the maximum value of the smoothed ith eigenperiod $\langle T_i \rangle$ during the earthquake, see figure 4. The smoothing operation smears out the local peaks, when the structure enters the plastic range.Explicit expressions for the damage localization were developed for the 2-dimensional case.

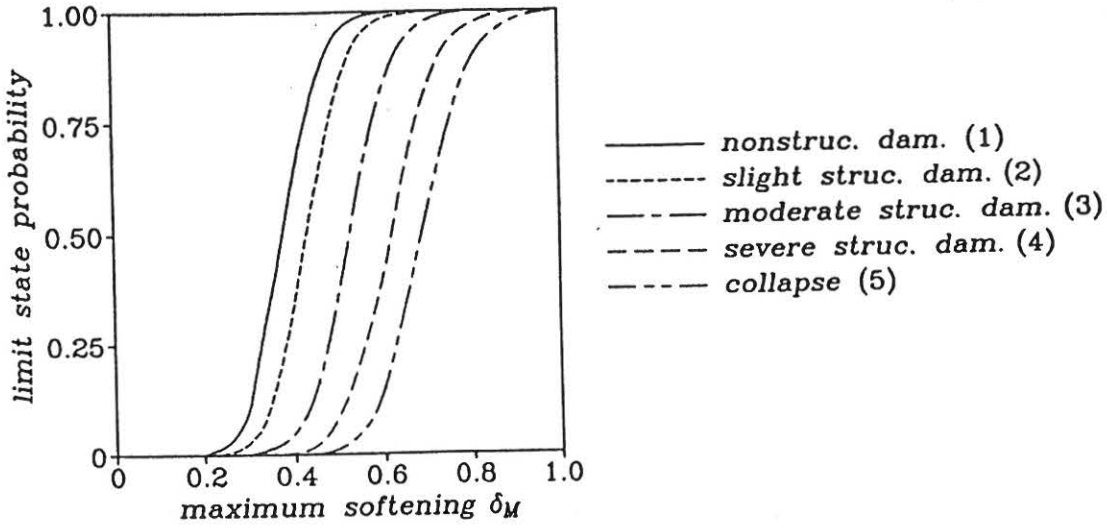

Figure 3: Distribution function of observed limit state values of global maximum softening reported by DiPasquale et al. [4].

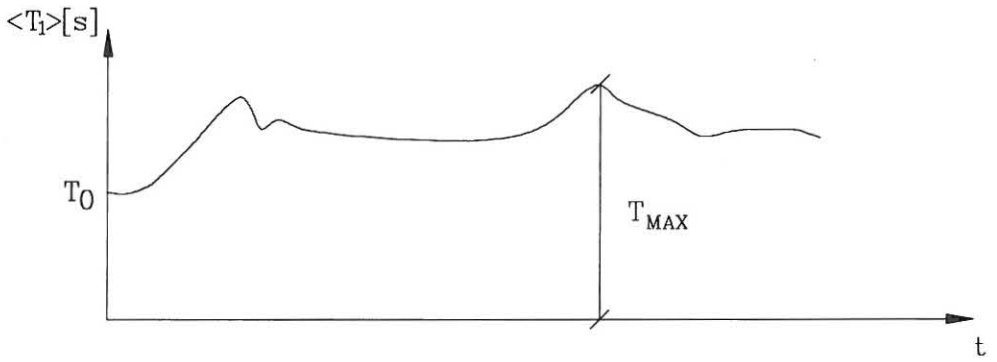

Figure 4: Definition of maximum value of the fundamental eigenperiod.

It is clear from the definition of this index that in case the maximum softening is 0 no damage has occurred in the structure, and $MSDI = 1$ indicates a total loss of global stiffness in the structure.

Local Softening Damage Index (LSDI)

The local softening damage index has recently been suggested by Skjærbæk et al. [16], as still another extension of the maximum softening damage principle.

The local softening damage index $LSDI_i(t)$ for substructure i is defined from

$$\mathbf{K}_{i,e}(t) = (1 - LSDI_i(t))^2 \, \mathbf{K}_{i,0} \tag{10}$$

where $\mathbf{K}_{i,0}$ is the initial undamaged stiffness matrix of the substructure and $\mathbf{K}_{i,e}(t)$ is the stiffness matrix of an equivalent linear substructure for which the summation over all substructures

$$\mathbf{K}_e(t) = \sum_{i=1}^{n} \mathbf{K}_{i,e}(t) \tag{11}$$

produces an equivalent global stiffness matrix $\mathbf{K}_e(t)$. $LSDI_i(t)$ is then identified so that $\mathbf{K}_e(t)$ produces exactly the measured smoothed eigenfrequencies $\langle f_i(t) \rangle$ at a given time t. As possible substructures a part of the structure, a storey or even a single beam element may be considered. Normally only the two lowest smoothed eigenfrequencies can be identified due to lack of energy at higher frequencies in the ground motions.
The $LSDI_i(t)$ for each storey is solved from the equation

$$\left(\mathbf{K}_e(t) - (\langle f_i(t) \rangle)^2 \mathbf{M}\right) \mathbf{\Phi}_i(t) = \mathbf{0} \tag{12}$$

Since normally more than two LSDIs have to be dermined, these cannot be determined uniquely if only two eigenfrequencies are identified, and a special technique has to be used. The method used here is thoroughly described in Skjærbæk et al. [16], [17].

Estimation of input parameters

From the previously presented damage indicators it is seen that three different types of input are required in order to evaluate the various damage indicators.

1. Displacement time series
2. Displacement and restoring force time series
3. Eigenfrequency time series

In the following the methods applied for estimation of these quantities are presented.

Identification of storey displacements and restoring forces

Time Integration

In order to evaluate the displacements or velocities from measured acceleration time series, one or two time integrations of the acceleration response become necessary. In reality, however, measured acceleration data contain spurious response components caused by uncontrolled phenomena associated with the structure/system being studied and the measurement/recording system itself. These noisy components of the record can significantly alter the character of the velocity and displacement histories obtained by successive integration.
In order to eliminate these phenomena the acceleration signal is bandpass filtered to cut very low and high frequency components out of the signal before integration. After the first integration the velocity response is obtained and a new bandpass filtering is performed before the last integration to obtain the displacement response.

Estimation of Shear Force-Interstorey Deformation Curves

From the acceleration measurement at each storey the shear force-interstorey deformation curve can be estimated for each storey. The restoring shear force is calculated in a spring-mass model of the structure using the acceleration data. The corresponding interstorey deformations are obtained from the noise threatened integration of the acceleration data. The shear

force-interstorey deformation curve is estimated from this information using a least squares interpolation technique.

Using a multi-degree-of-freedom mass-spring model with one lateral degree of freedom assigned at each measuring point (storey), where the storey mass m_i is lumped, the dynamic equilibrium expression will be on the form

$$P_i(t) = \sum_{j=i}^{N} m_j \ddot{y}_j(t) \tag{13}$$

for each interval between the storeys. $P_i(t)$ is the shear force in the storey below mass i, N is the total number of masses, m_i is the mass of storey i and $\ddot{y}_i(t)$ is the measured total acceleration at storey i. The shear forces can then be calculated inserting the measured accelerations into (13).

I should be noted, that this method is only effective for structures with deformation behaviour as the one to the left in figure 5, where the relative displacement directly displays the deformation behaviour, rather than the one to the right, where the displacements are effected by large axial strains in the columns.

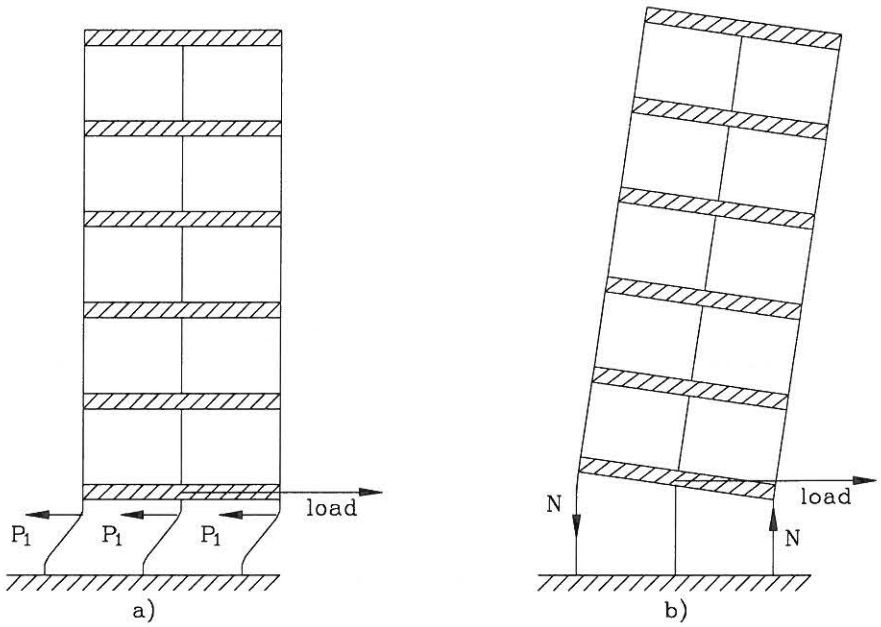

Figure 5: Relative displacement versus deformation response of frame and shear wall structures.

Identification of frequencies and mode shapes using recursive ARMAV

The frequencies and mode shapes of the degrading structure are estimated using ARV (AutoRegressive Vector) and ARMAV (AutoRegressive Moving Average Vector) models, see Kirkegaard et al. [6], [7]. In the case where the structure is time-varying due to the introduction of damage a recursive implementation of the ARMAV model is used. The presentation in the following is for the time-varying case.

Continuous Time Equivalent Linear Systems

In the continuous time domain an equivalent n-degree-of-freedom linear elastic viscous damped vibrating system is described by a system of linear differential equations of second order with

constant mass matrix $\mathbf{M}$, and slowly varying equivalent damping and stiffness matrices $\mathbf{C}_e(t)$, $\mathbf{K}_e(t)$ excited by the ground surface acceleration $\ddot{u}_g(t)$. Then the equations of motion for the equivalent linear multivariate system can be expressed as

$$\mathbf{M}\ddot{\mathbf{y}}(t) + \mathbf{C}_e(t)\dot{\mathbf{y}}(t) + \mathbf{K}_e(t)\mathbf{y}(t) = -\mathbf{M}\mathbf{b}\ddot{u}_g(t) \tag{14}$$

The state vector model corresponding to the dynamic equation (14) is

$$\dot{\mathbf{z}}(t) = \mathbf{A}(t)\mathbf{z}(t) + \mathbf{B}\ddot{u}_g(t), \quad \mathbf{z}_t = \begin{bmatrix} \mathbf{x}(t) \\ \dot{\mathbf{x}}(t) \end{bmatrix} \tag{15}$$

$$\mathbf{A}(t) = \begin{bmatrix} \mathbf{0} & \mathbf{I} \\ -\mathbf{M}^{-1}\mathbf{K}_e(t) & -\mathbf{M}^{-1}\mathbf{C}_e(t) \end{bmatrix}, \quad \mathbf{B} = \begin{bmatrix} \mathbf{0} \\ \mathbf{I} \end{bmatrix}$$

It is assumed that the system matrix $\mathbf{A}(t)$ is so slowly varying with time that the following applies

$$\mathbf{A}(t) \simeq \mathbf{U}(t)\boldsymbol{\mu}(t)\mathbf{U}^{-1}(t) \tag{16}$$

$$\mathbf{U}(t) = \begin{bmatrix} \mathbf{u}_1(t) & \dots & \mathbf{u}_{2n}(t) \\ \mu_1(t)\mathbf{u}_1(t) & \dots & \mu_{2n}(t)\mathbf{u}_{2n}(t) \end{bmatrix}$$

$\boldsymbol{\mu}(t) = \text{diag}[\mu_i(t)]$, $i = 1, 2, ..., 2n$. $\mathbf{U}(t)$ is the matrix whose columns contain the slowly varying eigenvectors of $\mathbf{A}(t)$. $\mu_i(t)$ is the time-varying eigenvalues of $\mathbf{A}(t)$. If the damping matrix admits modal decomposition the slowly varying circular frequency $\langle\omega_i(t)\rangle$ and the damping ratio $\zeta_i(t)$ of the ith mode can be obtained for underdamped systems from a complex conjugate pair of eigenvalues as

$$\left.\begin{matrix} \mu_j(t) \\ \mu_j^*(t) \end{matrix}\right\} = -\langle\omega_j(t)\rangle\zeta_j(t) \pm i\langle\omega_j(t)\rangle\sqrt{1-\zeta_j^2(t)} \tag{17}$$

Notice here, that (17) is always approximately fulfilled in case of lightly damped systems with well separated circular eigenfrequencies, Nielsen [10]. The time continuous equivalent system (14) is next replaced by an equivalent linear difference equation for which the system identification is performed.

Discrete Time ARMAV Model

For multivariate time series, described by an n-dimensional vector $\mathbf{y}(t)$, an ARMAV(p, q) model can be written with p AR-matrices and q MA-matrices

$$\mathbf{y}(t) + \sum_{i=1}^{p} \mathbf{A}_i(t)\mathbf{y}(t-i) = \sum_{j=1}^{q} \mathbf{B}_j\mathbf{e}(t-j) + \mathbf{e}(t) \tag{18}$$

where t now describes an integer valued non-dimensional time parameter. $\mathbf{A}_i(t)$ is an $n \times n$ matrix of autoregressive coefficients and $\mathbf{B}_j$ is an $n \times n$ matrix containing the moving average coefficients. $\mathbf{e}(t)$ is the model residual vector, an n-dimensional white noise vector sequence of the discrete time t.

In order to estimate the time-varying system it is necessary to estimate the parameters in the ARMAV-model (18) on-line. This is done using the Recursive Prediction Error Method (RPEM), see e.g. Ljung [8].

Evaluation of Modal Parameters

From the evaluated series of the model parameters in (18) the modal parameters of the continuous systems at each time step can be evaluated in the following way.

A discrete state-space equation for equation (18) is given by, see e.g. Pandit et al. [11]

$$\mathbf{Z}_t = \mathbf{F}_t \mathbf{Z}_{t-1} + \mathbf{W}_t \tag{19}$$

with the state vector $\mathbf{Z}_t$ identical to

$$\mathbf{Z}_t = \begin{bmatrix} \mathbf{y}(t) \\ \mathbf{y}(t-1) \\ \vdots \\ \mathbf{y}(t-p+1) \end{bmatrix} \tag{20}$$

and the time varying system matrix $\mathbf{F}_t$ given by

$$\mathbf{F}_t = \begin{bmatrix} -\mathbf{A}_1(t) & -\mathbf{A}_2(t) & \dots & -\mathbf{A}_{p-1}(t) & -\mathbf{A}_p(t) \\ \mathbf{I} & \mathbf{0} & \dots & \mathbf{0} & \mathbf{0} \\ \vdots & \vdots & \dots & \vdots & \vdots \\ \mathbf{0} & \mathbf{0} & \dots & \mathbf{I} & \mathbf{0} \end{bmatrix} \tag{21}$$

$\mathbf{W}_t$ includes the MA terms of the ARMAV model and takes the form

$$\mathbf{W}_t = \begin{bmatrix} \mathbf{e}(t) + \sum_{j=1}^{q} \mathbf{B}_j \mathbf{e}(t-j) \\ \mathbf{0} \\ \vdots \\ \mathbf{0} \end{bmatrix} \tag{22}$$

It is assumed that $\mathbf{F}_t$ can be decomposed as

$$\mathbf{F}_t = \mathbf{L}_t \boldsymbol{\lambda}_t \mathbf{L}_t^{-1} \tag{23}$$

$$\mathbf{L}_t = \begin{bmatrix} \mathrm{l}_1(t)\lambda_1^{p-1}(t) & \mathrm{l}_2(t)\lambda_2^{p-1}(t) & \dots & \mathrm{l}_{pn}(t)\lambda_{pn}^{p-1}(t) \\ \mathrm{l}_1(t)\lambda_1^{p-2}(t) & \mathrm{l}_2(t)\lambda_2^{p-2}(t) & \dots & \mathrm{l}_{pn}(t)\lambda_{pn}^{p-2}(t) \\ \vdots & \vdots & \dots & \vdots \\ \mathrm{l}_1(t) & \mathrm{l}_2(t) & \dots & \mathrm{l}_{pn}(t) \end{bmatrix} \tag{24}$$

$\boldsymbol{\lambda}_t = \mathrm{diag}[\lambda_i(t)]$, $i = 1, 2, .., pn$ is a diagonal matrix containing the discrete time-varying eigenvalues of $\mathbf{F}_t$ and $\mathbf{L}_t$ is a time-varying matrix whose columns contain the time-varying eigenvectors

$$\begin{bmatrix} l_i(t)\lambda_i^{p-1}(t) \\ l_i(t)\lambda_i^{p-2}(t) \\ l_i(t)\lambda_i^{p-3}(t) \\ \vdots \\ l_i(t) \end{bmatrix} \tag{25}$$

of the time varying matrix $\mathbf{F}_t$.

The discrete state space model can now be used for identification of modal parameters and scaled mode shapes as follows. The discrete eigenvalues of $\mathbf{F}_t$ are estimated by solving the eigenvalue-problem $\det(\mathbf{F}_t - \boldsymbol{\lambda}_t\mathbf{I}) = 0$ at each time step t which gives the pn discrete eigenvalues $\lambda_i(t)$. The continuous eigenvalues are obtained from $\mu_i(t) = \ln(\lambda_i(t))$ which implies that the modal parameters can be estimated using (17). The eigenvectors are determined directly from the the columns of the bottom $n \times pn$ submatrix of $\mathbf{L}_t$.

Experimental Results

Description of the Tests

The tests were conducted as shaking table tests as shown in figure 6.

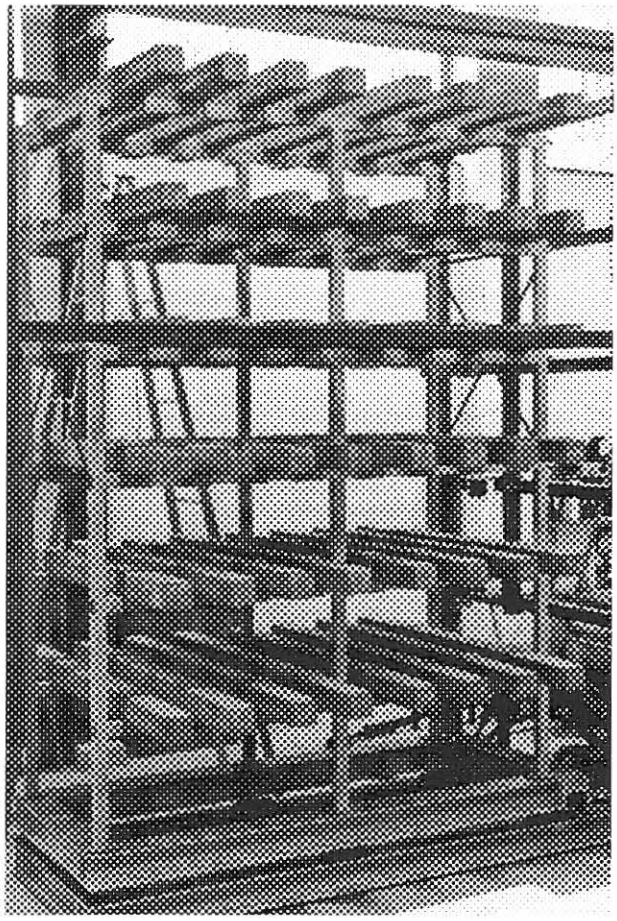

Figure 6: Photo of the test set-up.

As seen from figure 6 the frames were tested in pairs of two, where the storey weights are modelled by placing RC-beams in span between the two frames. Each of the two frames were

instrumented with a Brüel and Kjær accelerometer at each storey and one placed at the base to measure the ground motions. The force was provided by a 63 kN HBM cylinder with a ± 20 mm displacement. In figure 7 a schematic view of the test set-up is shown.

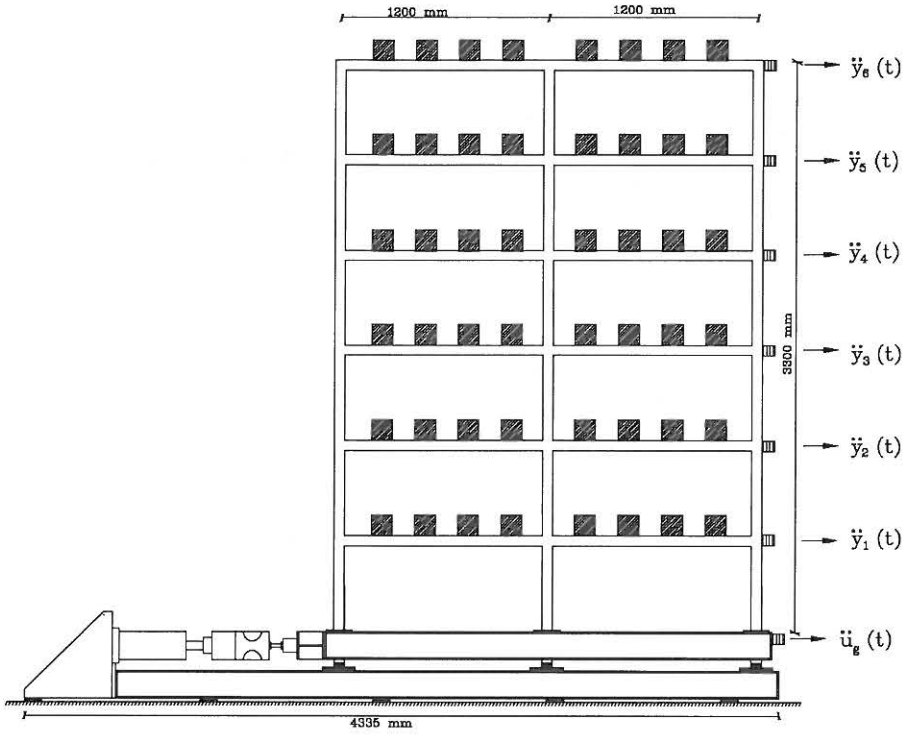

Figure 7: Side view of experimental set-up.

The frames were cast in-situ and consist of beams and columns with cross-sections of 50 by 60 mm. The beams are reinforced with 4ø6 KS410 ribbed steel bars with an average yield strength of 600 MPa. The concrete used had a strength of 20 MPa. The columns are reinforced with 6ø6 KS410 bars, see figure 8.

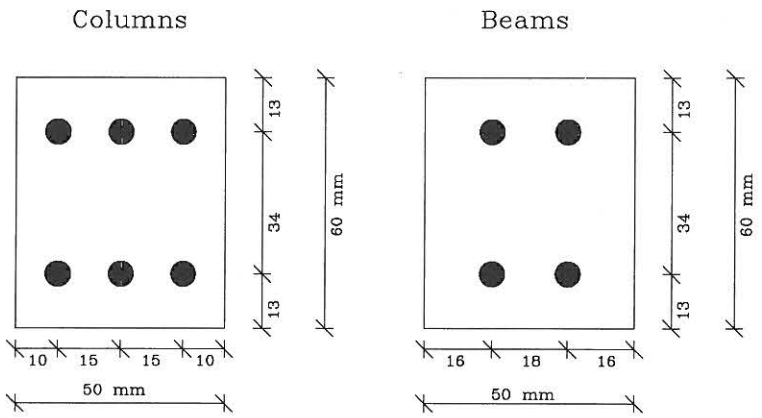

Figure 8: Cross-section of beam and columns.

The storey height is 0.55 m giving the model a total height of 3.3 m. Each of the two bays is 1.2 m wide giving the model a total width of 2.4 m. At each storey 8 0.12×0.12 RC-beams of

length 2m are placed between the two parallel frames to model the storey weights giving the model a total weight of approximately 40 kN.

During the tests the test set-up is subjected to two sequential earthquake like ground motions with increasing magnitude. The realizations are obtained by filtering amplitude modulated Gaussian white noise through a Kanai-Tajimi filter, see Tajimi [21]. The dominant frequency in the Kanai-Tajimi filter was chosen to be close to the lowest natural frequency of the undamaged structure. Each of the ground motion series had a length of 20 seconds.

Dynamic Testing

The dynamic test performed on the frame can be divided into two main categories:

1. Non-destructive testing
2. Destructive testing

The non-destructive testing is performed by means of free decay tests with well defined initial values from which the modal parameters of the structure are identified. Free decay tests are performed on the virgin structure and on the structure after each of the earthquake events. The destructive testing is performed applying two sequences of ground motion to the model test structure. In the following the results of the performed tests are presented.

Free Decay Tests

Free decay tests were performed by applying a force of 0.50 kN at the top storey which was suddenly released. During the free oscillations of the structure the storey accelerations were measured for a 20 second period. The measured top storey acceleration response from the free decay tests is shown in figure 9a in the case of the undamaged structure. In figures 9b and 9c the corresponding results of the free decay tests performed after the first and second earthquake sequence are shown.

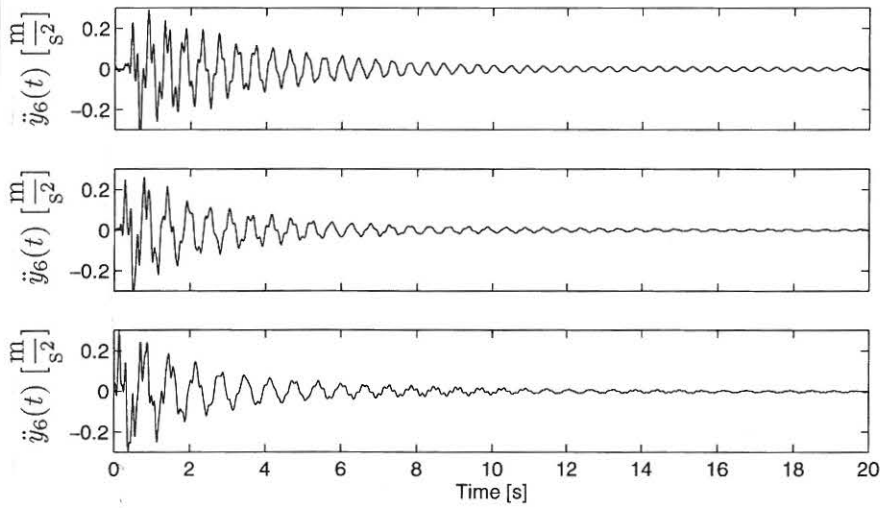

Figure 9: Measured top storey accelerations from pull-out test. a) Undamaged frame. b) After EQ1. c) After EQ2.

From the figure 9 it is clearly seen that the frequencies of the structure have changed significantly during the two strong motion events. In order to evaluate the modal parameters of the structure,

the free decay test time series were analysed using an ARV model and the modal parameters shown in table 1 were obtained.

State	f_1 [Hz]	f_2 [Hz]	ζ_1 [%]	ζ_2 [%]
Undamaged	2.15	6.95	1.7	1.4
After EQ1	1.79	6.13	2.9	2.5
After EQ2	1.48	5.38	3.8	2.9

Table 1: *Estimated modal parameters.*

Shaking Table Tests

During the strong motion shaking table tests the model test structure was exposed to two sequential time series of increasing magnitude labelled EQ1 and EQ2, respectively. EQ1 has a maximum ground surface displacement of 4 mm and EQ2 has a maximum displacement of 8 mm.

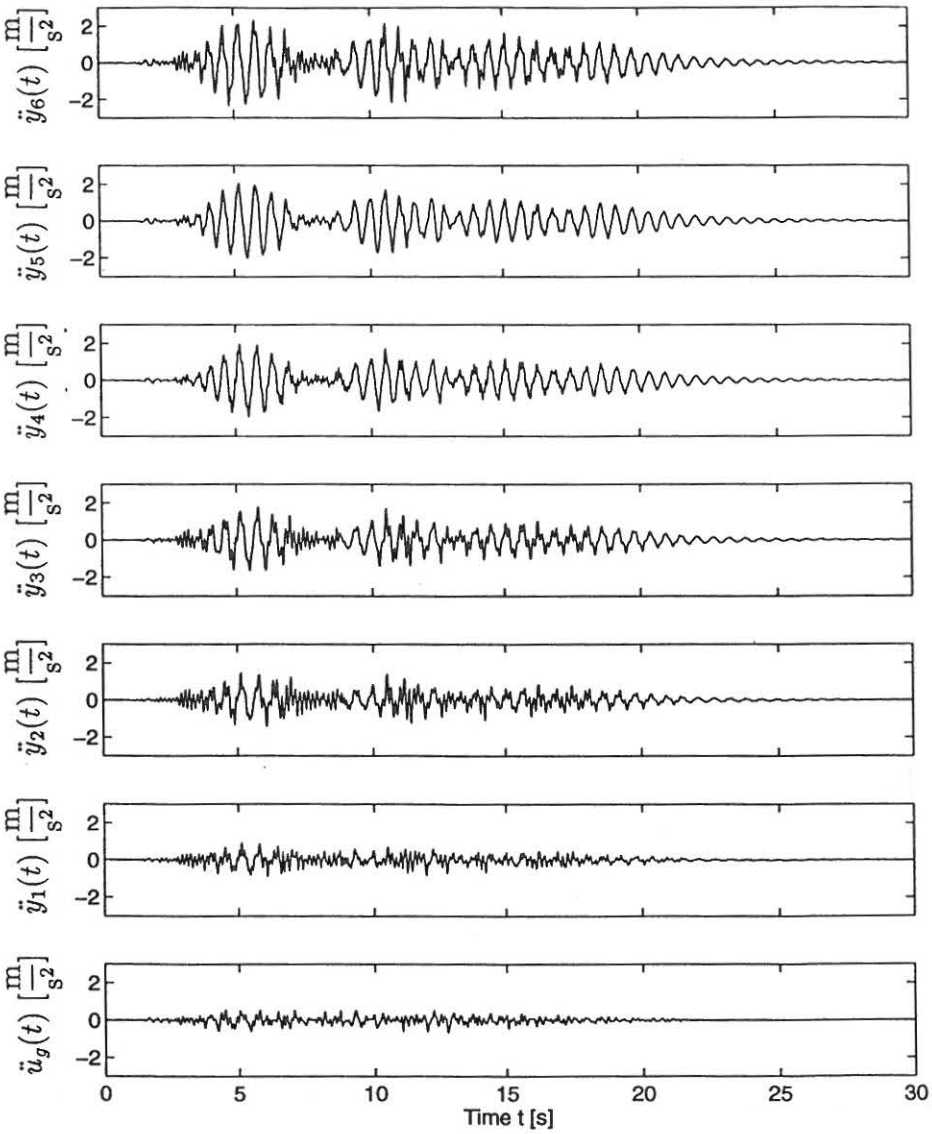

Figure 10: Measured accelerations during EQ1.

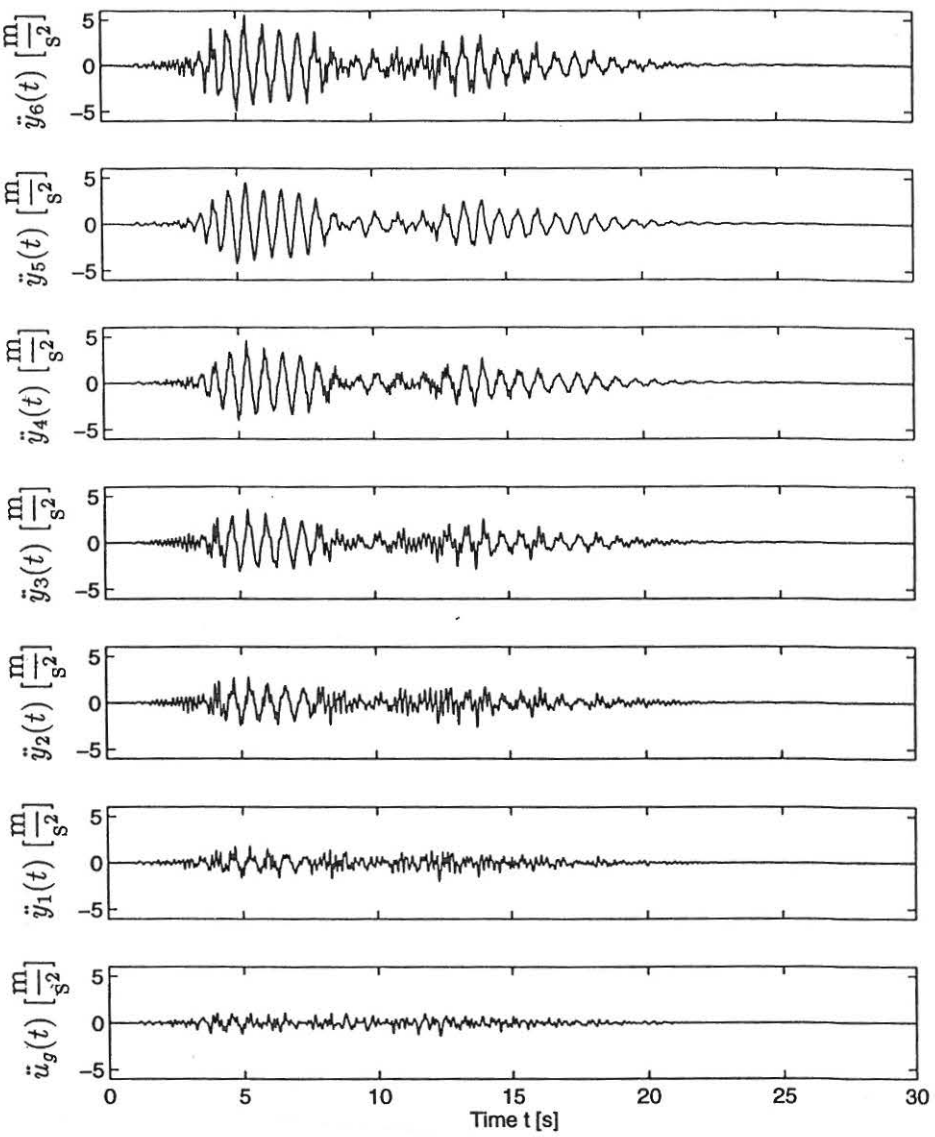

Figure 11: Measured accelerations during EQ2.

Processed data

This section presents processed data where top-storey displacements, frequency developments and force-deformation curves have been found using the procedures described earlier. During the integration process for obtaining the displacement process a Butterworth 6th order high-pass digital filter with a cut-off frequency of 0.5 Hz and a Butterworth 8th order low-pass digital filter with a cut-off frequency of 20 Hz have been used.

The top storey displacements during EQ1 and EQ2 are shown in figure 12a and 12b, respectively.

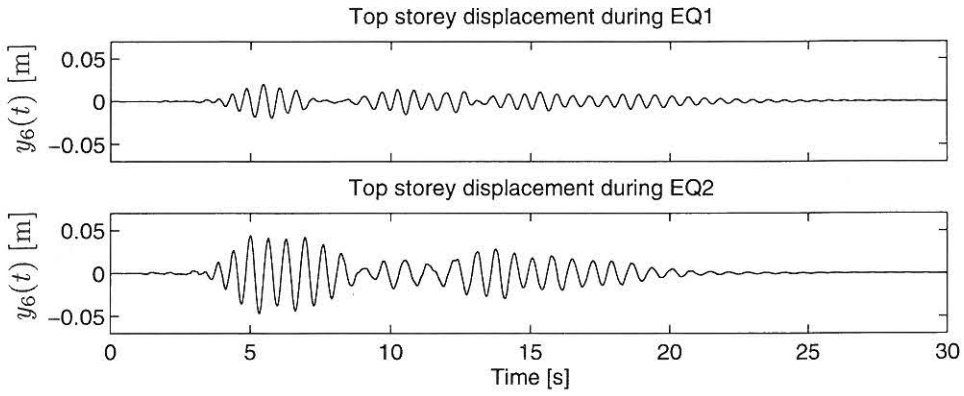

Figure 12: Top storey displacements during EQ1 and EQ2.

By considering the top storey displacements it is seen that the maximum displacement occurs already after a few cycles in both EQ1 and EQ2. Since several large amplitude cycles occur afterwards, the methods based on maximum displacements only are likely to give a poor damage assessment due to the introduction of low cycle fatigue.
The development in the two lowest eigenfrequencies during EQ1 and EQ2 is shown in figures 13 and 14, respectively.

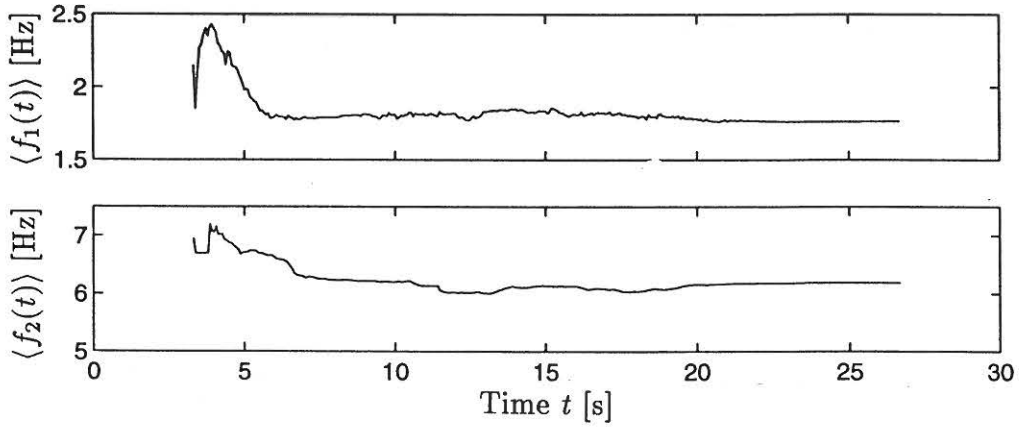

Figure 13: Development of smoothed natural frequencies in first and second mode during EQ1.

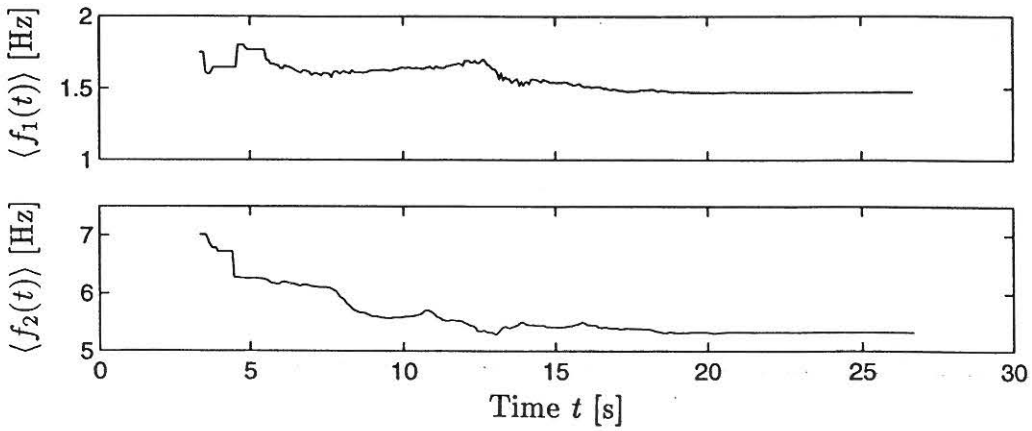

Figure 14: Development of smoothed natural frequencies in first and second mode during EQ2.

From the frequency time series presented in figures 13 and 14 the minimum values of the frequencies during the two earthquakes are extracted as shown in table 2 where also the maximum softening damage indicator is evaluated. In principle the curves in figure 14 should start at the ordinates where the curves in figure 13 end. The deviation is due to uncertainty in the frequency estimates in the initial part of the time series.

Earthquake	$f_{M,1}$ [Hz]	$f_{M,2}$ [Hz]	$\delta_{M,1}$	$\delta_{M,2}$
EQ1	1.76	6.00	0.18	0.14
EQ2	1.46	5.28	0.32	0.24

Table 2: *Maximum softenings.*

Comparing the evaluated maximum softenings with figure 3 it is seen that the damage incurred by the structure mainly seems to affect the first mode, where the largest softening is seen. The numerical values of the maximum softenings indicate that the structure after EQ1 only suffers from non-structural damage, and after EQ2 it enters into the light to moderate damage area. In figures 15-16 the shear force-interstorey deformation curves obtained for each of the storeys during the two earthquakes are shown using the previously described spring-mass model.

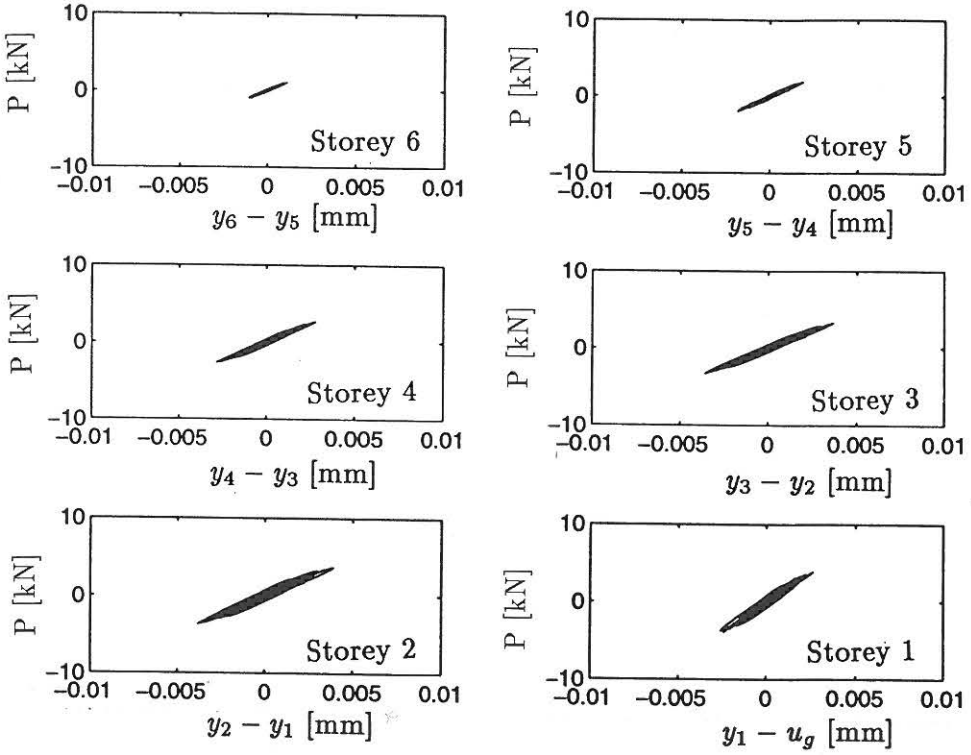

Figure 15: Force-deformation curves during EQ1.

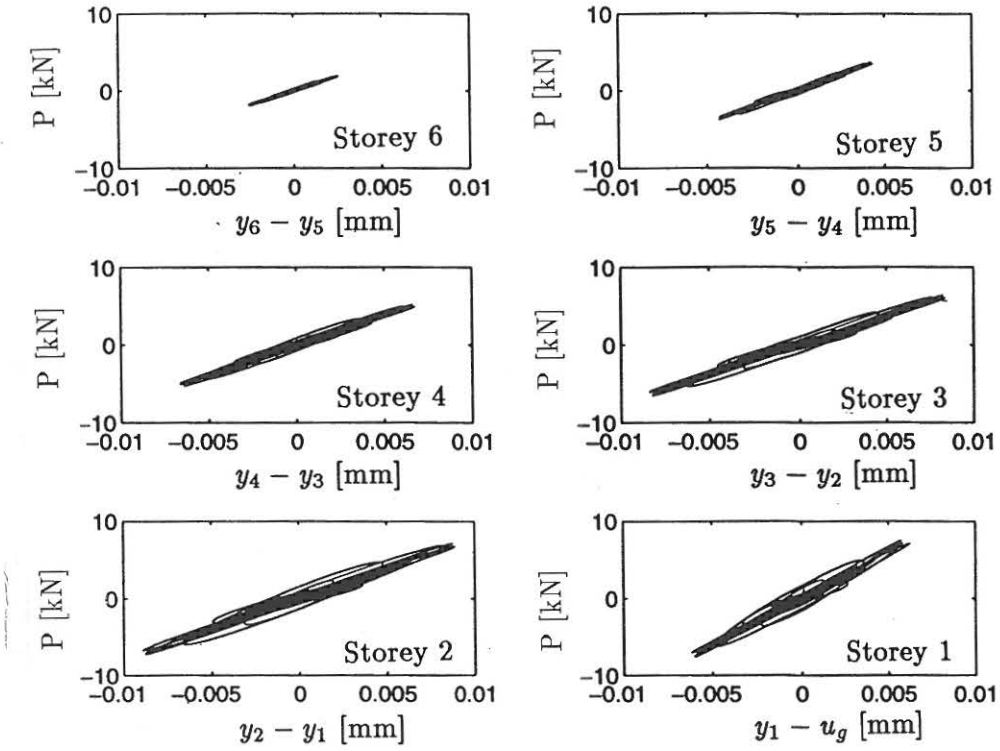

Figure 16: Force-deformation curves during EQ2.

From the figures 15-16 it is clearly seen that the main hysteresis occurs in the three lower storeys.

Static Testing

After the last of the dynamic tests one of the two frames was cut into smaller pieces at the mid-point of beams and columns. The cutting was performed using a high speed diamant based cutting devise. Half-beams and columns were subjected to a static test where a force was applied at the end of the beam or column. Corresponding values of force and displacement were sampled for forces in the range of 0.0-1.0kN for the columns and in the range of 0.0-0.4kN for the beams. A schematic view of the test set-up is shown in figure 17 and photos of the test set-up can be seen in figure 19.

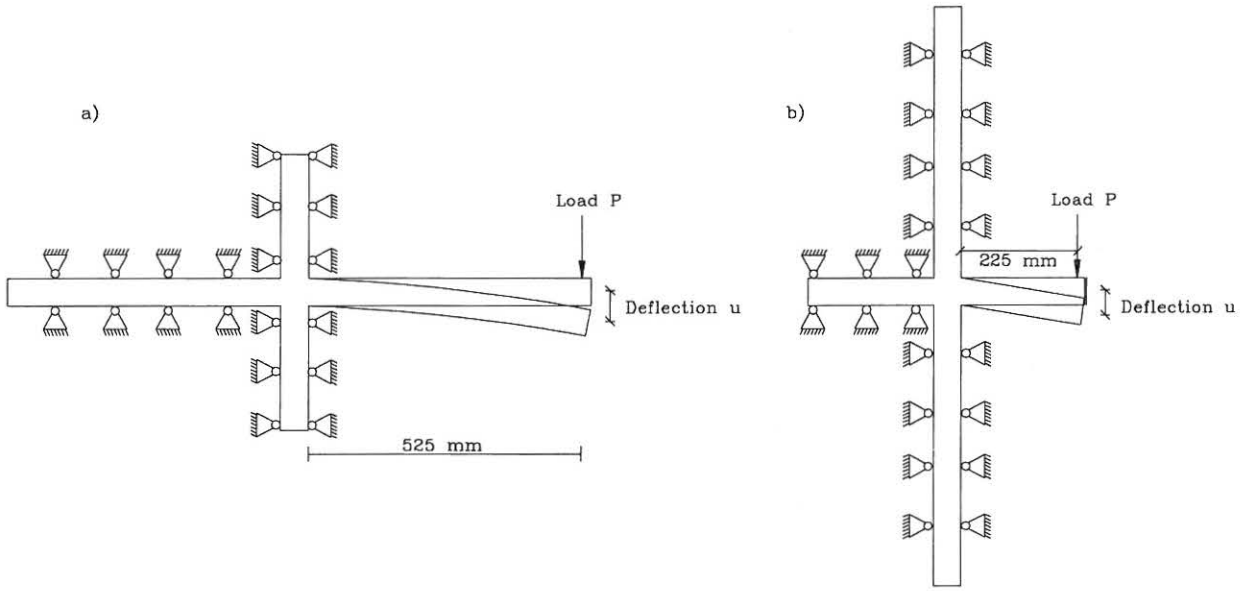

Figure 17: Schematic view of the test set-up used for the static testing. a) Set-up for beams. b) Set-up for columns.

Based on the static tests performed with each of the beams and columns the lateral stiffness can be estimated. In the following investigations only the initial tangent stiffness k_i of the obtained force-deformation curves of beams and columns is considered, see figure 18.

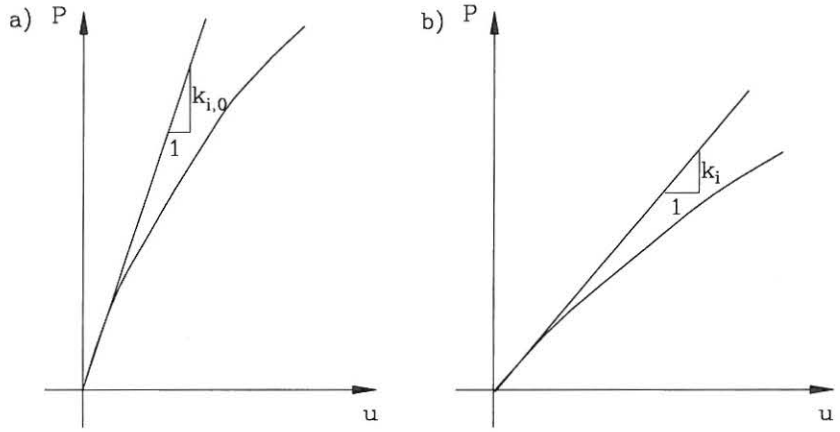

Figure 18: Force-deformation curves and definition of initial stiffness for beam or column no. i. a) Undamaged element. b) Damaged element.

As reference an undamaged frame was undergoing the same process of cutting and static testing to evaluate the corresponding undamaged initial stiffness $k_{i,0}$ for the beams and columns, see figure 18.
A damage index for beam or column no. i can then be defined as

$$ST_i = 1 - \sqrt{\frac{k_i}{k_{i,0}}} \tag{26}$$

It should here be noted that this damage index is consistent with the formulation used for the maximum and the local softening damage indices. The ST_i damage index is considered as the "true" measure of damage and the other damage indices are evaluated relative to this.

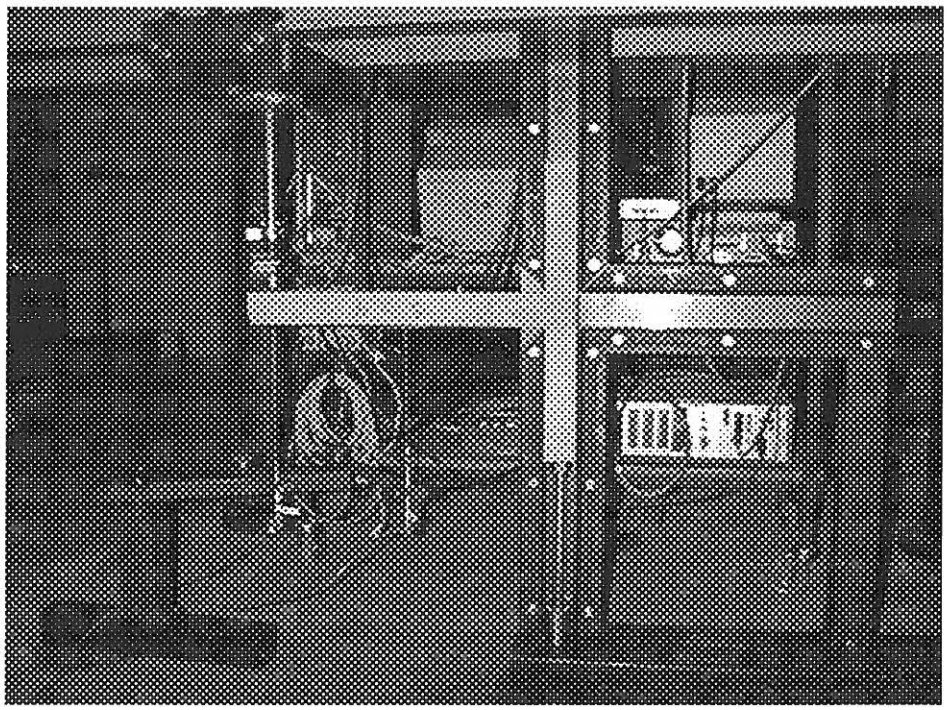

Figure 19: Photo of the static test setup.

Weighting of Local DI's

Each of the half beam damage indices is weighted into one storey damage index using the following method by Park et al. [13]

$$D_g^{DI} = \frac{\sum_{i=1}^{n} D_i^2}{\sum_{i=1}^{n} D_i} \tag{27}$$

It should be noted that (27) is only one of multiple possible weighting methods that can be used to calculate a global damage index from local damage indices. Further, there is no unique mapping from the local to the global damage. The weights could also be assigned from such considerations that lower storeys are more important than upper storeys, columns are more important than beams, etc.

Evaluated Damage Indicators

From figures 13 and 15 the damage indices after the first sequence of strong ground motions can be calculated. The results after EQ1 and EQ2 have been indicated in tables 3 and 4.
The results were obtained using a failure inter-storey drift of 3 per cent. Further, the parameter $\beta = 0.25$ was used in Park and Ang's index and the parameter $b = 0.77$ in Stephen's extended index SEI.

From table 3 it is seen that the ductility ratio DR predicts the first and second storeys to be slightly damaged after EQ1, whereas the storeys 3-6 have a ductility ratio less than 1 indicating that no yielding has occurred. In table 4 it is seen that the ductility ratio has increased significantly in the three lower storeys after EQ2 and also to some extent in the fourth and fifth storeys. The flexural damage ratio FDR predicts basically identical damage in the storeys 1-5 and the sixth storey to be almost undamaged after EQ1. Notice, that a flexural damage ratio of 1 indicates that no stiffness change has occurred, see (5). This tendency is

Storey	1st	2nd	3rd	4th	5th	6th
$ID_{T\&Y}$	0.0037	0.0056	0.0052	0.0041	0.0026	0.0015
DR	1.02	1.03	0.95	0.74	0.48	0.28
FDR	0.88	0.89	0.90	0.91	0.92	0.96
NCD	4.77	4.84	3.94	3.29	2.06	1.43
NDE	4.16	4.91	3.62	2.49	0.78	0.28
$P\&A$	0.18	0.30	0.26	0.19	0.11	0.06
SEI	0.06	0.10	0.07	0.06	0.02	0.00
$LSDI$	0.22	0.22	0.21	0.07	0.06	0.06

Table 3: *Damage indices after EQ1.*

Storey	1st	2nd	3rd	4th	5th	6th
$ID_{T\&Y}$	0.0113	0.0162	0.0152	0.0121	0.0078	0.0046
DR	3.11	2.98	2.79	2.21	1.42	0.85
FDR	0.71	0.75	0.76	0.75	0.76	0.84
NCD	15.9	15.11	12.34	10.05	5.99	3.92
NDE	32.34	32.84	23.85	16.57	5.15	1.72
$P\&A$	0.80	1.18	0.96	0.70	0.36	0.19
SEI	0.23	0.44	0.28	0.20	0.08	0.04
$LSDI$	0.43	0.37	0.23	0.13	0.12	0.12
ST	0.27	0.31	0.25	0.24	0.22	0.22

Table 4: *Damage indices after EQ2.*

also seen after EQ2 where the first storey incures the highest and the sixth storey the smallest damage. However, being solely based on the observed shear stiffness at the time of maximum deformation the index is likely to provide a poor estimation of damage in the present case. As seen in figure 12 the maximum deformation occurs at an early stage in both of the earthquake sequences, but several cycles with large deformation occur later in the sequences causing low cycle fatigue damage which is not captured by the FDR. Basically the three interstorey drifts considered are all scaled parameters of the maximum deformation observed in each of the storeys. The interstorey drift by Toussi and Yao, $ID_{T\&Y}$, shows an increasing damage with increasing earthquake intensity and indicates the second storey to be the most damaged. The cumulative normalized plastic deformation, NCD, and the cumulative normalized dissipated energy, NDE, both indicate the first and second storeys as the two most damaged storeys, the third and fourth storeys are indicated to be slightly less damaged and the fifth and sixth storeys are almost undamaged. This tendency is seen after both EQ1 and EQ2. The Park and Ang index, $P\&A$, predicts the highest damage level in the second storey after EQ1 as well as after EQ2 and only the fifth and sixth storeys are estimated to have a relatively low damage level. The same tendency is seen for the extended index, SEI, by Stephens. The local softening damage index, $LSDI$, indicates the three lower storeys to be basically identically damaged after EQ1. After EQ2 the $LSDI$ indicates the first storey to be most damaged followed by the second and third storeys. However, when estimating this index it should be noted that only measurements at the top storey are requested, whereas the remaining damage indicators require measurements at all storeys. The storey damage indicators ST_i obtained from the static tests of the beams and columns after EQ2 indicate the highest damage level to be present in the second storey closely followed by the first floor.

Comparing the damage indices in tables 3 and 4 based on interstorey displacements ($ID_{T\&Y}$, $P\&A$) with the remaining indices a pronounced deviation is noticed in the damage predictions for the first storey. The reason for this is the significantly larger stiffness of this storey due to the constraints at the supports. For the ductility ratio DR this has been partly compensated by the normalization with respect to the yield displacement.

Conclusions

The paper deals with damage assessment of a model test frame based on measured strong motion response. As reference damage/true damage the results of static testing are used. The damage assessment performed on the model test reinforced concrete frame using various response based damage indicators proposed in the literature indicates some divergence between the indicators. In the considered case it is especially found that the indicators based solely on maximum deformations provide a poor damage assessment due to several large amplitude cycles after the maximum deformation has occurred. A relatively newly suggested damage indicator estimated from only one global response is found in the present case to be competitive to traditional indicators.

Acknowledgement

The present research was partially supported by The Danish Technical Research Council within the project: **Dynamics of Structures**.

References

[1] Banon, H., Biggs, J. M. and Irvine, H. M., *Seismic Damage in Reinforced Concrete Frames.* Journal of the Structural Division, Proc., ASCE, Vol. 107, No. ST9, Sept. 1981, pp 1713-1729.

[2] Banon, H., and Veneziano, D., *Seismic Safety of Reinforced Concrete Members and Structures.* Earthquake Engineering and Structural Dynamics, Vol. 10, 1982, pp. 179-193.

[3] Culver, C.G. et al., *Natural Hazards Evaluation of Excisting Buildings.* Report no. BSS 61, National Bureau of Standards, U.S. Department of Commerce, 1975.

[4] DiPasquale, E. and Çakmak, A. Ş. *Detection of Seismic Structural Damage using Parameter-Based Global Damage Indices.* Probabilistic Engineering Mechanics, Vol. 5, No. 2, pp. 60-65, 1990.

[5] DiPasquale, E. and Çakmak, A. Ş. *Damage Assessment from Earthquake Records.* Structures and Stochastic Methods, Elsevier, Amsterdam, pp. 123-138.

[6] Kirkegaard, P.H., P. Andersen and R. Brincker, *Identification of the Skirt Piled Gulfaks C Gravity Platform using ARMAV Models.* Proceedings of the 14th IMAC, Dearborn, Michigan, USA, February 12-15, 1996.

[7] Kirkegaard, P.H., Skjærbæk, P.S. and Andersen, P., *Identification of Time-Varying Civil Engineering Structures using Multivariate Recursive Time Domain Models.* Proceedings of the 21st international Symposium on Noise and Vibrations, ISMA21, Leuven, Belgium, September 18-20, 1996.

[8] Ljung, L., *System identification - Theory for the user.* Prentice Hall, 1987.

[9] Nielsen, S.R.K. and Çakmak, A.Ş., *Evaluation of Maximum Softening Damage Indicator for Reinforced Concrete Under Seismic Excitation.* Proceedings of the First International Conference on Computational Stochastic Mechanics. Ed. Spanos and Brebbia, pp. 169-184, 1992.

[10] Nielsen, S.R.K., *Svingningsteori, bind I. Lineær svingningsteori.* Aalborg Tekniske Universitetsforlag, 1993.

[11] Pandit, S.M. and Wu, S.M., *Time Series and Systems Analysis with Applications.* Wiley and Sons, 1983.

[12] Park, Y.J. and Ang, A. H.-S., *Mechanistic Seismic Damage Model for Reinforced Concrete.* ASCE J. Struc. Eng., 111(4) April 1985, pp.722-739.

[13] Park, Y.J., Ang, A. H.-S., and Wen, Y.K., *Seismic Damage Analysis of Reinforced Concrete Buildings.* ASCE J. Struc. Eng., 111 (4) April 1985, pp. 740-757.

[14] Rahman, S. and Grigoriu, M., *A Markov Model for Local and Global Damage Indices in Seismic Analysis.* NCEER-94-0003 technical report, February 1994.

[15] Roufaiel, M.S.L. and Meyer, C., *Analysis of Damaged Concrete Frame Buildings.* Technical Report no. NSF-CEE-81-21359-1, Columbia University, New York, New York, 1983.

[16] Skjærbæk, P.S., Nielsen, S.R.K. and Çakmak, A.S., *Assessment of Damage in Seismically Excited RC-Structures from a Single Measured Response.* Proceedings of the 14th IMAC, Dearborn, Michigan, USA, February 12-15, 1996, pp. 133-139.

[17] Skjærbæk, P.S., Nielsen, S.R.K. and Çakmak, A.S., *Identification of Damage in RC-Structures from Earthquake Records - Optimal Location of Sensors.* Journal of Soil Dynamics and Earthquake Engineering, No. 6, Vol. 15, 1996, pp. 347-358.

[18] Sozen, M.A., *Review of Earthquake Response of Reinforced Concrete Buildings with a view to Drift Control.* State-of-the-Art-in-Earthquake-Engineering, 1981, Turkish National Commitee on Earthquake Engineering, Istanbul, Turkey, pp. 383-418.

[19] Stephens, J.E. and Yao, J.P.T., *Damage Assessment using Response Measurements.* ASCE J. Struc. Eng. 113 (4) April 1987, pp. 787-801.

[20] Stephens, J.E., *Structural Damage Assessment Using Response Measurements.* Ph.D.-thesis, Purdue University, 1985.

[21] Tajimi, H. *Semi-Empirical Formula for the Seismic Characteristics of the Ground.* Proceedings of the 2nd World Conference on Earthquake Engineering, Vol. II, 781-798, Tokyo and Kyoto.

[22] Toussi, S. and Yao, J.P.T., *Hysteresis Identification of Existing Structures.* ASCE J. Eng. Mech., Vol. 109, No. 5, Oct. 1983. pp. 1189-1203.

[23] Williams, M.S. and Sexsmith, R.G., *Seismic Damage Indices for Concrete Structures: A State-of-the-Art Review.* Earthquake Spectra, Vol. 11, No. 3, 1995, pp. 319-349.

FRACTURE AND DYNAMICS PAPERS

PAPER NO. 67: J. C. Asmussen, R. Brincker: *Estimation of Frequency Response Functions by Random Decrement.* ISSN 1395-7953 R9532.

PAPER NO. 68: P. H. Kirkegaard, P. Andersen, R. Brincker: *Identification of an Equivalent Linear Model for a Non-Linear Time-Variant RC-Structure.* ISSN 1395-7953 R9533.

PAPER NO. 69: P. H. Kirkegaard, P. Andersen, R. Brincker: *Identification of the Skirt Piled Gullfaks C Gravity Platform using ARMAV Models.* ISSN 1395-7953 R9534.

PAPER NO. 70: P. H. Kirkegaard, P. Andersen, R. Brincker: *Identification of Civil Engineering Structures using Multivariate ARMAV and RARMAV Models.* ISSN 1395-7953 R9535.

PAPER NO. 71: P. Andersen, R. Brincker, P. H. Kirkegaard: *Theory of Covariance Equivalent ARMAV Models of Civil Engineering Structures.* ISSN 1395-7953 R9536.

PAPER NO. 72: S. R. Ibrahim, R. Brincker, J. C. Asmussen: *Modal Parameter Identification from Responses of General Unknown Random Inputs.*ISSN 1395-7953 R9544.

PAPER NO. 73: S. R. K. Nielsen, P. H. Kirkegaard: *Active Vibration Control of a Monopile Offshore Structure. Part One - Pilot Project.* ISSN 1395-7953 R9609.

PAPER NO. 74: J. P. Ulfkjær, L. Pilegaard Hansen, S. Qvist, S. H. Madsen: *Fracture Energy of Plain Concrete Beams at Different Rates of Loading.* ISSN 1395-7953 R9610.

PAPER NO 75: J. P. Ulfkjær, M. S. Henriksen, B. Aarup: *Experimental Investigation of the Fracture Behaviour of Reinforced Ultra High Strength Concrete.* ISSN 1395-7953 R9611.

PAPER NO. 76: J. C. Asmussen, P. Andersen: *Identification of EURO-SEIS Test Structure.* ISSN 1395-7953 R9612.

PAPER NO. 77: P. S. Skjærbæk, S. R. K. Nielsen, A. Ş. Çakmak: *Identification of Damage in RC-Structures from Earthquake Records - Optimal Location of Sensors.* ISSN 1395-7953 R9614.

PAPER NO. 78: P. Andersen, P. H. Kirkegaard, R. Brincker: *System Identification of Civil Engineering Structures using State Space and ARMAV Models.* ISSN 1395-7953 R9618.

PAPER NO. 79: P. H. Kirkegaard, P. S. Skjærbæk, P. Andersen: *Identification of Time Varying Civil Engineering Structures using Multivariate Recursive Time Domain Models.* ISSN 1395-7953 R9619.

PAPER NO. 80: J. C. Asmussen, R. Brincker: *Estimation of Correlation Functions by Random Decrement.* ISSN 1395-7953 R9624.

PAPER NO. 81: M. S. Henriksen, J. P. Ulfkjær, R. Brincker: *Scale Effects and Transitional Failure Phenomena of Reinforced concrete Beams in Flexure. Part 1.* ISSN 1395-7953 R9628.

PAPER NO. 82: P. Andersen, P. H. Kirkegaard, R. Brincker: *Filtering out Environmental Effects in Damage Detection of Civil Engineering Structures.* ISSN 1395-7953 R9633.

PAPER NO. 83: P. S. Skjærbæk, S. R. K. Nielsen, P. H. Kirkegaard, A. Ş. Çakmak: *Case Study of Local Damage Indicators for a 2-Bay, 6-Storey RC-Frame subject to Earthquakes.* ISSN 1395-7953 R9639.

FRACTURE AND DYNAMICS PAPERS

PAPER NO. 84: P. S. Skjærbæk, S. R. K. Nielsen, P. H. Kirkegaard, A. Ş. Çakmak: *Modal Identification of a Time-Invariant 6-Storey Model Test RC-Frame from Free Decay Tests using Multi-Variate Models.* ISSN 1395-7953 R9640.

PAPER NO. 85: P. H. Kirkegaard, P. S. Skjærbæk, S. R. K. Nielsen: *Identification Report: Earthquake Tests on 2-Bay, 6-Storey Scale 1:5 RC-Frames.* ISSN 1395-7953 R9703.

PAPER NO. 86: P. S. Skjærbæk, S. R. K. Nielsen, P. H. Kirkegaard: *Earthquake Tests on Scale 1:5 RC-Frames.* ISSN 1395-7953 R9713.

PAPER NO. 87: P. S. Skjærbæk, S. R. K. Nielsen, P. H. Kirkegaard, A. Ş. Ç nak: *Experimental Study of Damage Indicators for a 2-Bay, 6-Storey RC-Frame.* ISSN 1395-7953 R9725.

PAPER NO. 88: P. S. Skjærbæk, S. R. K. Nielsen, P. H. Kirkegaard, A. Ş. Çakmak: *Damage Localization and Quantification of Earthquake Excited RC-Frames.* ISSN 1395-7953 R9726.

PAPER NO. 89: P. S. Skjærbæk, P. H. Kirkegaard, S. R. K. Nielsen: *Shaking Table Tests of Reinforced Concrete Frames.* ISSN 1395-7953 R9704.

PAPER NO. 90: J.C. Asmussen, R. Brincker: *A new Approach for Predicting the Variance of Random Decrement Functions.* ISSN 1395-7953 R9723.

PAPER NO. 91: P. S. Skjærbæk, P. H. Kirkegaard, G. N. Fouskitakis, S. D. Fassois: *Non-Stationary Modelling and Simulation of Near-Source Earthquake Ground Motion: ARMA and Neural Network Methods.* ISSN 1395-7953 R9641.

PAPER NO. 92: J. C. Asmussen, S. R. Ibrahim, R. Brincker: *Application of Vector Triggering Random Decrement.* ISSN 1395-7953 R9634.

PAPER NO. 93: S. R. Ibrahim, J. C. Asmussen, R. Brincker: *Theory of Vector Triggering Random Decrement.* ISSN 1395-7953 R9635.

PAPER NO. 94: R. Brincker, J. C. Asmussen: *Random Decrement Based FRF Estimation.* ISSN 1395-7953 R9636.

PAPER NO. 95: P. H. Kirkegaard, P. Andersen, R. Brincker: *Structural Time Domain Identification (STDI) Toolbox for Use with MATLAB.* ISSN 1395-7953 R9642.

PAPER NO. 96: P. H. Kirkegaard, P. Andersen: *State Space Identification of Civil Engineering Structures from Output Measurements.* ISSN 1395-7953 R9643.

PAPER NO. 97: P. Andersen, P. H. Kirkegaard, R. Brincker: *Structural Time Domain Identification Toolbox - for Use with MATLAB.* ISSN 1395-7953 R9701.

PAPER NO. 98: P. S. Skjærbæk, B. Taşkin, S. R. K. Nielsen, P. H. Kirkegaard: *An Experimental Study of a Midbroken 2-Bay, 6-Storey Reinforced Concrete Frame subject to Earthquakes.* ISSN 1395-7953 R9706.

PAPER NO. 99: PAPER NO. 98: P. S. Skjærbæk, S. R. K. Nielsen, P. H. Kirkegaard, B. Taşkin: *Earthquake Tests on Midbroken Scale 1:5 Reinforced Concrete Frames.* ISSN 1395-7953 R9712.

Department of Building Technology and Structural Engineering
Aalborg University, Sohngaardsholmsvej 57, DK 9000 Aalborg
Telephone: +45 9635 8080 Telefax: +45 9814 8243